SECTION 89

MICROWAVE EMISSION CHARACTERISTICS OF SEA ICE

by

A. T. Edgerton and G. Poe
Microwave Division
Aerojet-General Corporation
El Monte, California

ABSTRACT

The National Atmospheric and Oceanic Administration is sponsoring research concerning the microwave emission characteristics of sea ice. Initial analyses were concerned with modeling of sea ice emission and multiwavelength microwave measurements obtained north of Point Barrow, Alaska during June 1970 by Goddard Space Flight Center (GSFC). These data show that ice-water boundaries are readily discernible. A major result of this work was the general classification of sea ice brightness temperatures into categories of "high" (~240°K) and "low" (~200 - 210°K) emission corresponding to young and weathered sea ice respectively. Also, a sea ice emission model was developed which allows variations of ice salinity and temperature in directions perpendicular to the ice surface but neglects lateral variations and nonspecular surface and volume scattering effects. This model does not adequately account for the apparent bi-modal emission characteristics of sea ice.

The sea ice research has since been extended to include development of more adequate sea ice emission models and comparison of the refined models with more extensive sea ice measurements obtained by GSFC in the vicinity of the 1971 AIDJEX Camp. This work is now in progress.

INTRODUCTION

This paper describes sea ice research performed by Aerojet-General Corporation. This study, sponsored by the National Environmental Satellite Service of NOAA, is concerned with the analysis of microwave radiometric measurements of sea ice. The study was prompted, in part, by the need for an effective means of mapping sea ice conditions in the presence of the adverse arctic weather.

Specific objectives of the study include: (1) analysis of multi-frequency microwave emission characteristics of different sea ice types; (2) evaluation of attenuation (and re-radiation) at microwave frequencies of the arctic atmosphere; and (3) determination of the feasibility of mapping sea ice types and ice-water boundaries using microwave radiometry.

Experimental data used in the first phase of the sea ice study were obtained over the Beaufort Sea north of Point Barrow, Alaska during June 1970. Data were obtained by the Goddard Space Flight Center (GSFC) with instrumentation installed in a Convair 990. Instrumentation aboard the aircraft included a 1.55-cm (19.35 GHz) microwave imager, eight microwave radiometers, infrared radiometers (10 to 12 microns), various cameras, a laser geodolite, meteorological instrumentation, and various aircraft attitude and position sensors. Data were obtained at altitudes ranging from 115 m to 9 km. Data analysis was based entirely on information obtained with the aircraft.

Microwave measurements were compared with the available support data to determine the emission characteristics of the sea ice encountered during the overflight. Brightness temperature data were evaluated in terms of the dependence of microwave emission on observational wavelength, antenna viewing angle and antenna polarization.

A numerical model of microwave emission from vertically structured media was employed to evaluate the effects of variations in the brine content (neglecting volume scattering) and thermometric temperature of sea ice. A qualitative comparison of the computed and measured brightness temperatures indicates that a more complex model is needed to adequately describe microwave emission by sea ice.

The second phase of the study was initiated in January 1972. This activity is concerned with developing a more adequate sea ice emission model based, in part, on data obtained by GSFC in the vicinity of the 1971 AIDJEX Camp. Several mechanisms are presently being evaluated to explain the apparent "bi-modal" emission phenomena.

The writers wish to thank several individuals for their assistance and cooperation in this study. Drs. Nordberg, Gloersen and Wilheit of GSFC provided the aircraft data used in the study. Drs. A. Strong of NOAA and W. Campbell of the USGS were also helpful in identifying sea ice features encountered during the study. Dr. A. Strong also provided administrative and technical guidance during the study.

SEA ICE MEASUREMENTS

BACKGROUND

In June of 1970, GSFC conducted an aircraft mission to obtain microwave radiometric measurements of Arctic sea ice. The mission was carried out with Ames Research Center's Convair 990 aircraft. Multi-frequency microwave measurements were taken above a solid cloud cover at an altitude of 9 km (29,000 feet) along a flight track extending about 800 km due north of Point Barrow, Alaska, over the Beaufort Sea. On the return (southbound) leg of the flight, data were taken along the same track below the cloud cover at an altitude of approximately 125 meters (400 feet).

Microwave data derived from this flight were of good quality and correspond to a variety of sea ice features. Supporting data for the June flight include aerial photography, laser geodolite information, infrared temperature measurements (10 to 12 microns), meteorological and aircraft dynamics observations. Unfortunately, no supporting ice data (e.g., ice depth, temperature or salinity profiles, etc.) were taken along the flight track. Hence, the analysis of these data was based solely on the aircraft data.

AIRCRAFT INSTRUMENTATION

The sensor complement aboard the aircraft included a microwave imager, eight microwave radiometers, two infrared radiometers, two cameras and a laser profilometer. The infrared sensors consisted of a Barnes PRT-6 radiometer (10 to 12 microns) and an infrared temperature profile radiometer (ITPR) (10 to 11 microns). Photography was taken with a nadir-looking 70-mm camera equipped with infrared aero-ektachrome film and a 35-mm camera pointed out the left side of the aircraft 45° above nadir. Ice surface roughness data were acquired during the low level flight with a Spectra-Physics Model 3A laser geodolite.

Table I gives pertinent specifications of the microwave radiometers aboard the CV-990. The observational wavelengths of the sensors ranged from 3.2 cm (9.3 GHz) to 0.51 cm (58.8 GHz). The 1.55-cm (19.35 GHz) radiometer was the only microwave imager aboard the aircraft. The relatively large time constants utilized in the 1.35, 0.96, 0.56, 0.55, 0.51 and 2.81-cm measurements impeded detailed correlation with photographic data. The 1.55-cm imager data received primary consideration because of the excellent corresponding 70-mm downward-looking

photography. The 0.81-cm data were also of excellent quality but were difficult to correlate with surface features since the antenna beamprint (45° to the left of aircraft) was outside of the 70-mm camera's 65°30' field of view. As a result, the 0.81-cm data were correlated with visible surface variations using oblique photography from the 35-mm camera boresighted with the radiometer.

ATMOSPHERIC CONDITIONS AND DESCRIPTION OF SEA ICE ALONG FLIGHT TRACK

Point Barrow weather information for the month preceding the airborne microwave measurements was obtained from the Environmental Data Service of NOAA. During May 1970, the mean maximum and minimum temperatures were -5°C and -10°C, respectively. The extreme high temperature was +3.3°C on 30 May. The extreme low was -22.8°C on 4 May. Precipitation during May 1970 amounted to 0.03 mm, all in the form of snow. In the days just prior to the microwave measurements (6 June 1970) an intense storm of several days duration occurred over the Beaufort Sea which gave rise to subfreezing temperatures, some snowfall and presumably, renewed ice growth.

During the airborne measurements an almost solid stratus cloud deck persisted from 150 m to 600 m above the ice surface. Consequently, the supporting sea ice observations (aerial photography, surface temperature measurements, laser profiles, etc.) obtained on the high altitude (8.9 km) northbound flight had limited value in the present study. The supporting data obtained on the southbound low altitude (<150 m) return flight indicated that the air temperature ranged between -3 and -4°C (±3°C).

The available sea ice data for analyzing microwave brightness temperatures included (1) notes from sea ice observers aboard the CV990 aircraft, (2) surface temperature measurements, (3) aerial photographs and (4) laser geodolite measurements. Additional desirable (but unavailable) sea ice data include brine content, density and temperature profiles, internal ice structure and small scale surface roughness. The photographs and sea ice observer notes provided information concerning the ice types, snow cover, relative age of adjacent floes, weathering and deformation. The laser geodolite provided an uncalibrated measure of the intensity of the reflected laser signal and a direct measure of the surface relief.

The 70-mm photographs indicate that two varieties of sea ice were encountered over major portions of the flight track. These included ice of uniform appearance and conspicuously mottled (deformed) ice. The 70-mm photographs indicate that the mottled ice has experienced recent

deformation (ridging, rafting and fracturing) and is younger than the uniform textured ice. The uniform ice appears to have experienced some weathering (melting). The actual age of the two varieties of ice is uncertain, however, both types are though to be first year ice, the younger (mottled) ice being one month old or less (personal communications with W. Campbell and W. Weeks, 1970). Both varieties of ice occurred in floes ranging in size from a fraction of a kilometer to several tens of kilometers. The photographs and observer notes indicate that the uniform ice is covered with a veneer of snow of unknown thickness. The young ice also had a partial snow cover in the form of sastrugii (windblown snow ridges of about one-half meter height).

Minor occurrences of finger ice and open water were also encountered during the measurements. The finger ice occurred adjacent to polynyas and comprised a minor fraction of the flight track. The leads and polynyas were generally small and infrequent along the aircraft track.

The laser surface profile of the young sea ice floes indicate the presence of numerous angular ridges of the order of 0.5 to 1.3 meters high. The uniform floes contain low rounded, surface features of 20-cm or less height. These are believed to be weathered pressure ridges.

In summary, two distinct types of sea ice were encountered over major portions of the June 1970 mission. These will subsequently be termed (1) young ice and (2) weathered ice. The young ice was comparatively thin with extensive ridging and rafting, was probably one month old, or less, and showed no evidence of weathering (melting evidenced by rounded ridges, etc.). The weathered ice is of uniform appearance, has a generally smooth surface, and shows no signs of recent deformation.

Water and ice surface temperatures, determined with the ITPR during the low level (<150 m) measurements, ranged from 270.2 to 273.0°K and averaged about 272°K. Surface temperatures of 273°K were noted very infrequently along the flight track. Consequently, little or no liquid water should have occurred in the snow cover. At these temperatures melting can occur on the sea ice surface depending on the brine content of the ice. Unfortunately, no surface-based data are available and it is not possible to establish whether melting occurred. The sea ice was definitely not saturated (with melt water) since no melt ponds or conspicuous incipient melting were noted on the aerial photography (a few isolated ponds believed to be trapped sea water were noted on young ice floes in close proximity to buckling and rafting). Similarly, no definite statement can be made regarding the ice thickness. Estimates were attempted based on the apparent "free-board" of the floes, as determined from the geodolite observations. However, the resultant thicknesses were inconsistent and were not used in the analysis.

MICROWAVE MEASUREMENTS OF SEA ICE

General

The 1.55-cm imager data were reduced to color images and computer listings of brightness temperature versus antenna view angle (beam position). Data from the other microwave radiometers were generally reduced to computer-generated plots of brightness temperature versus time. All data (except for the 0.5 to 0.6-cm sensors) were examined collectively to determine the wavelength dependence of microwave emission by sea ice. Also, the 0.81-cm data were evaluated in terms of the polarization of sea ice emission, and the 1.55-cm data were examined in terms of emission versus view angle. Detailed comparisons between the two dominant sea ice features (young and weathered ice) were limited to the 0.81 and 1.55-cm data since these were the only data with sufficient spatial resolution.

Dual-Polarized 0.81-cm Brightness Temperatures

Dual-polarized 0.81-cm (37 GHz) microwave measurements were obtained with a side-looking radiometer oriented 45° to the left of nadir. Figure 1 presents representative data obtained in the time interval of 23:23:30 through 23:28:15. A cursory examination of Figure 1 shows that sea ice brightness temperatures are conspicuously bi-modal. Measured horizontally and vertically polarized temperatures for young (mottled) and weathered (uniform) ice are 230 and 240°K, and 180 and 190°K respectively. The sea ice data of Figure 1 exhibit approximately 10°K of polarization. These differences are somewhat greater when the radiometer calibration is taken into consideration. Also, note the substantial differences between open water (highly polarized with very low horizontally polarized brightness temperatures) and the radiometrically cool, comparatively unpolarized, weathered sea ice. These data indicate that dual-polarized measurements can be used to distinguish between the radiometrically cool weathered ice and partially beam-filling water.

Multiwavelength Brightness Temperatures

As mentioned previously, pronounced changes in low altitude 1970 Arctic microwave measurements occurred when viewing different ice types ("young" and "weathered") and when viewing ice-water boundaries. A comparison of these changes at different observational wavelengths reveals several interesting features, Figure 2. The observed contrasts in microwave emission of ice and water for a wavelength of 0.81 cm (and greater) are substantial (100 to 150°K). The greatest contrast occurs

at 2.8 cm. The reduced contrast in the vertical polarization at 0.81 cm is consistent with theoretical predictions. Also, note that the polarization differences are small when viewing the ice. These results present rather encouraging prospects for mapping ice-water boundaries with high altitude microwave measurements.

The multiwavelength contrast in observed brightness temperatures of "young" and "weathered" ice types is presented in Figure 3. The data at wavelengths greater than 0.55 cm exhibit similar responses to different ice types with the contrast increasing with decreasing wavelength. This phenomenon is presently inexplicable. The 0.81-cm data has more noise than the other odata since a shorter integration time was employed.

A graphical illustration of the contrast in emissivity of the two ice types is presented in Figure 4 as a function of observational wavelength. The change in emissivity $\Delta\epsilon$ (larger minus smaller) is presented to minimize effects of calibration errors. A surface temperature of 272°K consistent with infrared measurements has been used in computing $\Delta\epsilon$. Note that $\Delta\epsilon$ exhibits a substantial dependence on wavelength.

SEA ICE MODEL

GENERAL

Sea ice is a complex, dynamic substance. The microwave brightness temperatures of sea ice depend on such phenomena as brine content, thermometric temperature gradients, ice growth rate, internal ice structure, surface geometry as well as other physical sea ice properties. A sufficiently general theory of the microwave emission properties of sea ice which incorporates these phenomena does not presently exist. The recent theory of Stogryn[1] represents perhaps the most general treatment of the effects of basic physical phenomena on sea ice emission. The theory allows variations of the temperature and dielectric constant in the direction perpendicular to a substance's surface but neglects variations in directions parallel to the surface. Also, nonspecular surface scattering and volume scattering effects have necessarily been ignored. The necessity arises since a theory of scattering for situations in which the sizes of scattering centers or the dimensions of surface irregularities approach significant portions of the observational wavelength has not been derived at present. Thus scattering from brine pockets and possibly other structures in sea ice at microwave frequencies are presently unsolved problems.

In this section results of computations using the theory of Stogryn are given which illustrate the dependence of brightness temperature on salinity and thermal temperature of sea ice. These results are preceded by a brief outline of the theory and assumptions employed in the computations.

In the present considerations it is assumed that specifications of (1) the vertical profile of salinity and temperature and (2) the functional dependence of the dielectric constant with salinity, temperature and frequency completely determine the microwave emission of sea ice. Phenomena such as horizontal fluctuations of salinity and temperature, nonspecular scattering, and ice structure variations arising from growth history are completely ignored.

According to the theory of vertically structured media, the horizontally polarized brightness temperature at an angle of incidence θ and frequency ν is given by

$$T_h(\theta,\nu) = |R_h|^2 T_{sky}(\theta,\nu) + 4\left(\frac{2\pi\nu}{c}\right)^3 \cos\theta \int_{-\infty}^{o} dz' \, T(z') \mathrm{Im}\left[K(z',\nu)\right] |A(z')|^2 \tag{1}$$

where $T_{sky}(\theta,\nu)$ is the incident sky temperature, R_h the reflection coefficient of the surface for horizontally polarized radiation, c the free space speed of light, $T(z')$ the thermometric temperature at the depth z' below the surface, $K(z',\nu)$ the complex dielectric constant of the medium, and $A(z')$ is the value, at $z = 0$, of the solution of the differential equation

$$\frac{d^2a}{dz^2} + \left(\frac{2\pi\nu}{c}\right)^2 \left[K(z,\nu) - \sin^2\theta\right] a = -\delta(z - z') \tag{2}$$

satisfying the boundary conditions

$$\frac{da}{dz} - i\left(\frac{2\pi\nu}{c}\right) \cos\theta \; a = 0 \qquad \text{at} \quad z = 0 \tag{3a}$$

a is an outgoing wave as $z \to -\infty$ and, at the ice-water boundary $z = -E$

$$a(-E + 0) = a(-E - 0)$$

$$\left.\frac{da}{dz}\right|_{z=-E+o} = \left.\frac{da}{dz}\right|_{z=-E-o} \tag{3b}$$

The symbol Im [ ] in (1) signifies the imaginary part of the quantity enclosed in the brackets while, in (2), δ is the Dirac delta function and, in (3a), $i = \sqrt{-1}$. Similarly, the vertically polarized temperature is given by

$$T_v(\theta,\nu) = |R_v|^2 T_{sky}(\theta,\nu) + 4\left(\frac{2\pi\nu}{c}\right) \cos\theta \int dz' \, T(z') \, \mathrm{Im}\left[K(z',\nu)\right] \left[\left|\frac{dB}{dz'} + \left(\frac{dK}{dz'} \Big/ K\right) B\right|^2 + \left(\frac{2\pi\nu}{c}\right)^2 \sin^2\theta \, |B|^2\right] \quad (4)$$

where R_v is the reflection coefficient for vertically polarized radiation and B is the value, at $z = 0$, of the solution of the differential equation

$$\frac{d^2b}{dz^2} - \left(\frac{dK}{dz} \Big/ K\right) \frac{db}{dz} + \left(\frac{2\pi\nu}{c}\right)^2 \left[K(z,\nu) - \sin^2\theta\right] b = -\delta(z - z') \quad (5)$$

satisfying the boundary conditions

$$\frac{db}{dz} - i\left(\frac{2\pi\nu}{c}\right) \cos\theta \; K(0,\nu) \, b = 0 \qquad \text{at} \quad z = 0 \quad (6a)$$

b is an outgoing wave as $z \to -\infty$ and, at the ice-water boundary,

$$b(-E + 0) = b(-E - 0)$$

$$\frac{db}{dz} \Big/ K(z,\nu)\Big|_{z=-E+o} = \frac{db}{dz} \Big/ K(z,\nu)\Big|_{z=-E-o} \quad (6b)$$

A practical numerical procedure for determining R_h , R_v , A , and B when $K(z,\nu)$ is known is discussed by Stogryn. The major problems that arise in the application of (1) and (4) to the calculation of the ice brightness temperature are the specification of the temperature profile $T(z)$ and the dielectric constant $K(z,\nu)$.

The dielectric constant of salt water ice is controlled by its temperature and rate of formation. The temperature is important because the brine (liquid phase) content of salt water ice varies rapidly with temperature and does not vanish even at temperatures well below the freezing point. In addition, the brine volume is dependent on both the salinity of the water from which the ice is formed and on the rate of growth of the ice. Thus, since the dielectric properties of brine differ markedly from those of water in the solid phase, the dielectric constant of saline ice may be expected to show considerable sensitivity to environmental conditions.

Because of the complex nature of sea ice, experimental determinations of its dielectric properties at microwave frequencies would be extremely desirable. Unfortunately, these do not seem to be available. Of the measurements which are known to the authors, those of Addison[2], who determined the dielectric constant at frequencies up to 100 MHz, appear to be the most comprehensive. While Addison's measurements were conducted at frequencies which are much too low to be used for quantitative studies in the GHz region of the spectrum, his results do indicate a strong dependence of the dielectric properties of saline ice on temperature and salinity.

In the absence of measured values, it is necessary to rely on a theoretical formula for the dielectric constant. Thus, we assume that saline ice may be treated as a mixture of pure ice and brine and consider the problem of calculating the dielectric constant of the mixture. From among the available formulas, all of which must be used with caution, that of Wiener[3], which has often been used in studies of ice and snow (see, e.g., Evans[4]) was chosen. According to Wiener's formula, the dielectric constant of the mixture is

$$K = \frac{K_b\, pU + K_i(1 - p)}{pU + 1 - p} \tag{7}$$

where

$$U = \frac{K_i + f}{K_b + f} \tag{8}$$

In (7) and (8) K_b is the dielectric constant of the brine, K_i the dielectric constant of pure ice, p the brine volume (ratio of the volume occupied by the brine to the total volume of a small sample of saline ice), and f a form number which is determined by the shape of the brine cells. Since brine cells are roughly rod-like in shape, f is expected to be large. However, its precise value has not been determined previously and it must be considered to be an adjustable parameter for the purposes of this study.

The two dielectric constants, K_b and K_i, appearing in (7) and (8) have been studied in the GHz portion of the electromagnetic spectrum. According to Cumming[5], the real part of the dielectric constant of pure ice is 3.15 and independent of the temperature. Available evidence also indicates that it is independent of frequency in the GHz range. The imaginary part of the dielectric constant of the ice is temperature-dependent. However, its value is small compared to that of water and, since the present state of knowledge does not warrant a more detailed treatment, an average value of 3×10^{-3} will be used. Thus, we have

$$K_i = 3.15 + 3 \times 10^{-3} i \qquad (9)$$

The dielectric constant of brine may be computed as a function of frequency using formulas of the Debye form (Stogryn[6]) when the salinity and temperature of the brine is known. Equations for computing the brine volume p from a knowledge of salinity and temperature of sea ice are given by Stogryn[7].

RESULTS OF CALCULATIONS

On the basis of these equations and the theory presented, calculations of the brightness temperature of sea ice have been performed for a number of different models. In all cases, the models consisted of a layer of ice of uniform thickness over sea water. The ice temperature and salinity were assumed to be -1.99°C and 4°/oo respectively, at the ice-water boundary. The choice of 4°/oo for sea ice salinity at the ice-water boundary is consistent with published values. Trial calculations were also undertaken for salinity values of 8 and 12°/oo. These gave the same results, indicating that this parameter is not critical in the computations. In the various models, the temperature profile of the ice was assumed to vary linearly from the ice-water boundary to the ice-air boundary. Different salinity profiles were investigated. These included linear profiles and profiles in which the salinity varied from its surface value to a value of 12°/oo at a depth equal to one-tenth of the ice thickness, from which point it decreased linearly to its final value of 4°/oo. Calculations were also performed for total ice thicknesses of 10, 20, and 100 cm. In all cases which were investigated, the brightness temperature varied by only a fraction of a degree from that computed for a 10-cm-thick layer of ice having a linear salinity profile. This result is understandable on the basis of the large loss tangent of sea ice whose thermal temperature is close to 0°C. Hence, although the results to be presented below refer specifically to linear salinity profiles in 10-cm-thick ice, they are representative of many more complex structures.

Figures 5 and 6 show the results of calculations for frequencies of 19.4 GHz (λ = 1.55 cm) and 37 GHz (λ = 0.81 cm). In all cases it is assumed that the radiometers are close to the surface and the brightness temperatures include the effects of a model Arctic summer atmosphere which is essentially consistent with known conditions prevailing during the aircraft measurements. Computations are shown only for $\theta = 45^{\circ}$ for 37 GHz since this was the antenna viewing angle of the aircraft instrument. The 19.4 GHz plots include both $\theta = 0^{\circ}$ and $\theta = 45^{\circ}$. It is apparent from the figures that a rather large range of brightness temperatures may arise as a result of either surface temperature changes or salinity variations. These changes are especially rapid near 0°C where the brine volume of the ice increases rapidly with temperature.

Estimates of the electromagnetic power skin depth δ (depth of penetration) in sea ice were also undertaken using Equation (10) and Wiener's dielectric mixing formula. Im denotes taking the imaginary part and λ is the 5, 10 and 20 parts per thousand and temperatures of -1 through -30°C for an observational wavelength of 1.55 cm, Figure 7. Skin depth values are given in terms of free-space wavelengths. These data clearly indicate the strong dependence of microwave emission by sea ice near 0°C on near-surface phenomena.

$$\delta = \frac{\lambda}{4\pi \, \mathrm{Im}(\sqrt{K})} \qquad (10)$$

COMPARISON OF MEASUREMENTS AND THEORY

The microwave emission characteristics of sea ice are dependent on several parameters. These include (1) ice temperature, (2) salinity, (3) density, (4) ice thickness, (5) liquid water content, (6) internal structure, (7) surface roughness and (8) snow cover or surface water (if present). A model of vertically structured media has been applied with reasonable success in calculating the effects at 13.4 and 37 GHz of (1), (2), and (4) on sea water ice grown under laboratory conditions[7].

However, as noted earlier direct quantitative comparisons of measured brightness temperatures obtained during the overflights with those predicted by the above model could not be made in the present study since no information regarding the salinity and general condition of the sea ice was available. Preliminary evaluations of microwave measurements obtained during the 1971 AIDJEX Expedition where ice surface temperatures averaged about -20°C indicate that the existing vertically structured media model cannot account for the emission characteristics of weathered ice. Hence, alternate mechanisms must be examined to explain the bi-modal results.

Several alternatives are offered. First, if it is assumed that increases in nonspecular surface scattering increase the emissivity of sea ice, then the brightness temperatures of the "high" emission sea ice type may arise from the more complex surface structure of the young ice. Likewise, the temperature of the "low" emission ice type would be due to the lack of nonspecular scattering associated with the "smooth" surface of weathered ice.

A second explanation may be offered using the results noted by Addison in his dielectric constant measurements of saline ice. Although the measurements were carried out at frequencies (20 Hz to 100 MHz) lower than microwave frequencies, the phenomena observed may be applicable to microwave frequencies. Addison found in several instances that as the sea ice was subjected to changes in temperature (-10 to -22°C) the real part of the dielectric constant increased significantly (by a factor of 2 in one case). The effect was not observed in all cases but did occur often enough to be noted. Thus, if we consider weathered ice as having been recycled, the presently observed low brightness temperatures of weathered ice ("low" emission ice types) may be due to an increase in the dielectric constant. The phenomenon may be associated with drainage of brine from brine pockets in the ice.

Finally, it should be noted that although volume scattering arising from volume inhomogeneities (e.g., brine pockets, air bubbles, etc., in the ice) may explain the observed phenomenon, lack of theoretical results precludes making general intuitive statements similar to those presented above. The primary reason for considering volume scattering effects arises in the analysis of laboratory grown saline ice (Stogryn[7]) where it was found that the principal discrepancy between theory and experiment occurred at temperatures near 0°C. It was conjectured that scattering by large brine pockets in the ice invalidated the description of the dielectric constant by the simple mixing formula due to Wiener.

Preliminary analysis of acquired 1971 Arctic microwave measurements indicate that a similar bi-modal classification of sea ice emission occurred. Since the 1971 measurements were performed on ice whose temperatures were much lower than those occurring in the 1970 measurements (Nordberg[8]) (-20°C in 1971 versus 0°C in 1970), variations in brine volume as described by the existing vertically structured media model in ice appear unimportant in explaining the bi-modal emission character. Clearly a more complex model than presently available is needed to understand this phenomenon.

CONCLUSIONS AND CURRENT ACTIVITIES

CONCLUSIONS

The ultimate goal of the research reported herein is the development of a practical microwave remote sensing technique(s) for synoptic aerial and/or satellite mapping of general ice type, ice-water boundaries, ice thickness and related physical properties (e.g., salinity, temperature and density) of Arctic sea ice. An initial step toward this goal has been an integrated research program consisting of (1) numerical modeling of sea ice emission and (2) analysis of recently acquired multifrequency airborne passive microwave measurements.

In (1) the theory of vertically structured media (which incorporates subsurface salinity and temperature gradients and neglects nonspecular scattering) was employed to establish the dependence of sea ice emission on salinity and temperature for several observational wavelengths (2.81, 1.55, 1.35, 0.96, and 0.81 cm) and view angles (0 and 45 degrees from nadir). Utilizing linear distributions of salinity and temperature, it was found that a relatively large range of sea ice emissions (or brightness temperature) may arise as a result of either surface temperature or salinity changes. The computed sea ice emission exhibited the largest changes at temperatures near 0°C. (This phenomenon is due to the fact that changes in the brine volume in ice are especially rapid near 0°C.)

In (2) it was found that the observed low altitude (150 m) brightness temperatures of sea ice generally fell into two distinct ranges corresponding to "high" (240°K) and "low" (200°K). Since no "surface-truth" data were taken during the 1970 Arctic flights, photographic and laser data were utilized to identify the ice types. From all indications, the high and low brightness temperatures were respectively, young unweathered ice (thought to have formed within the past month or so) and relatively old ice which appeared to have undergone weathering (surface melting and refreezing). The contrast in brightness temperature between the two ice types decreased significantly as the observational wavelength increased. The mechanisms responsible for this phenomenon were not isolated during the first phase of this study although several possibilities were identified. A significant contrast in the brightness temperatures of ice and water was observed at all wavelengths greater than (or equal to) 0.81 cm. The contrast apparently increased with wavelength and was largest at 2.81 cm.

In summary, the present study presents rather encouraging prospects for aerial synoptic mapping of ice-water boundaries and identification of gross ice types (e.g., "young" versus "old") using passive microwave measurements.

CURRENT ACTIVITIES

Work is continuing toward development of an adequate numerical model of sea ice emission. This work is being guided by the aircraft and sea ice observations obtained during the 1971 AIDJEX Expedition. Modeling activities are focused on the effects of scattering due to brine cells, bubbles, crystal structure, surface roughness, etc.

REFERENCES

1. Stogryn, A., "The Brightness Temperature of a Vertically Structured Medium," Radio Science, Vol. 5, No. 12, pp 1397-1406, Dec. 1970.

2. Addison, J., "Electrical Properties of Saline Ice," J.A.P., Vol. 40, pp 3105-3114, 1969.

3. Wiener, O., "Leipziger Berichte," 62, p. 256, 1910.

4. Evans, S., "Dielectric Properties of Ice and Snow – A Review," J. of Glaciology, Vol. 5, pp 773-792, 1965.

5. Cumming, W., "The Dielectric Properties of Ice and Snow at 3.2 Centimeters," J.A.P., Vol. 23, pp 768-773, 1952.

6. Stogryn, A., "Equations for Calculating the Dielectric Constant of Saline Water at GHz Frequencies," IEEE Trans. MTT, Aug. 1971.

7. Stogryn, A., "The Brightness Temperature of Sea Ice," Interoffice Memo, Aerojet-General Corp., El Monte, Calif., 1970.

8. Nordberg, W., et al, "Measurements of Microwave Emission from a Foam Covered, Wind Driven Sea," NASA preprint X-650-70-384, 1970.

Table I

MICROWAVE RADIOMETERS FLOWN ON 1970 CV-990 MISSION
(all radiometers horizontally polarized unless otherwise noted)

Frequency (GHz)	Wavelength (cm)	View Angle (from Nadir)	3-dB Beamwidth (Deg)	RMS[3] (ΔT) (^{o}K)	Integ. Time (Sec)	Primary Experimentor
19.35[1]	1.55	±50^{o}	2.8	1.40	0.025	GSFC/AGC
22.235	1.35	0^{o}	10	0.3	2	MIT/JPL
31.4	0.955	0^{o}	10	0.4	2	MIT/JPL
53.65	0.559	0^{o}	10	1.2	2	MIT/JPL
54.90	0.546	0^{o}	10	0.6	2	MIT/JPL
58.80	0.510	0^{o}	10	0.7	2	MIT/JPL
9.3	3.23	180^{o}	13	1.0	1	JPL
10.69	2.81	0^{o}	7	0.6	2	JPL
31.4	0.955	180^{o}	10	0.9	1	JPL
37.0[2]	0.811	45^{o} left	5	0.5	Variable 0.01-1.0	AGC

1. Electrically scanned radiometer.

2. 37 GHz radiometer positioned 45^{o} above nadir to the left of the aircraft, dual polarized.

3. RMS values are given for one second integration time.

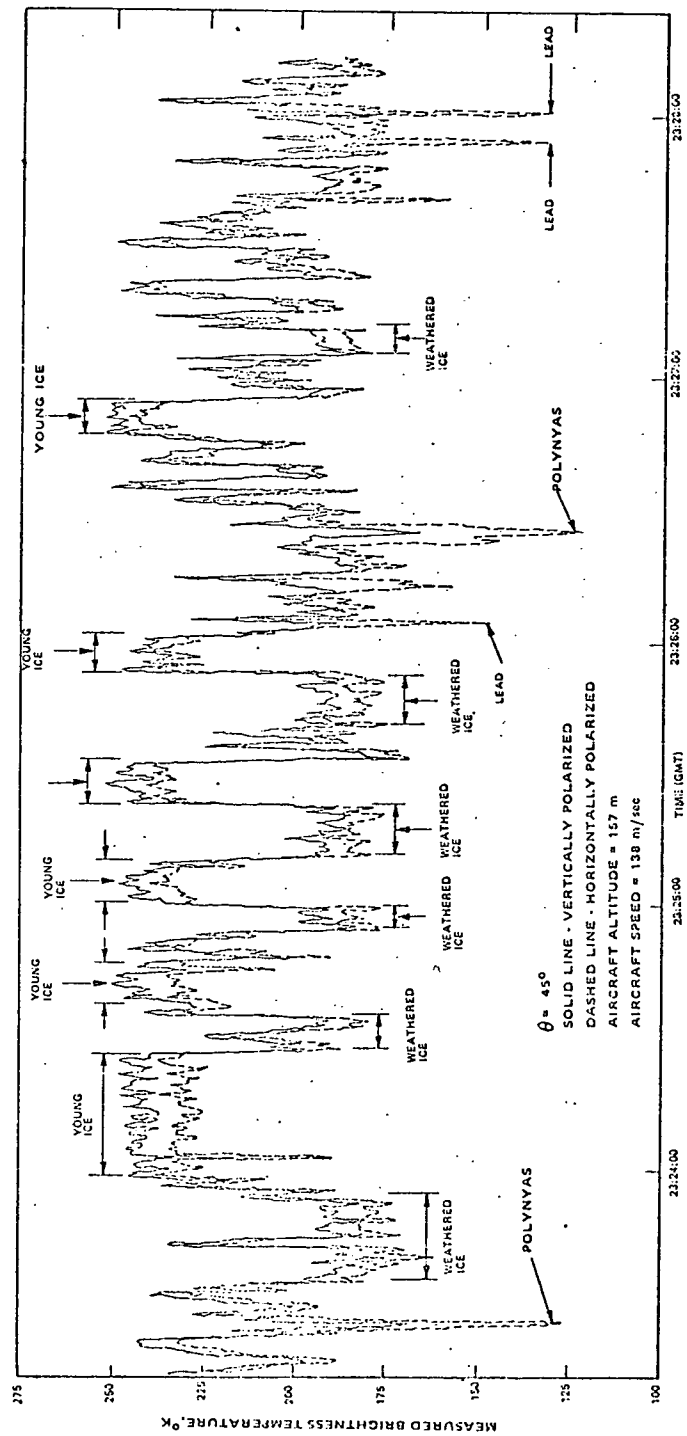

Figure 1. 8.1 mm (37 GHz) Brightness Temperature Measurements of Arctic Sea Ice, 11 June 1970

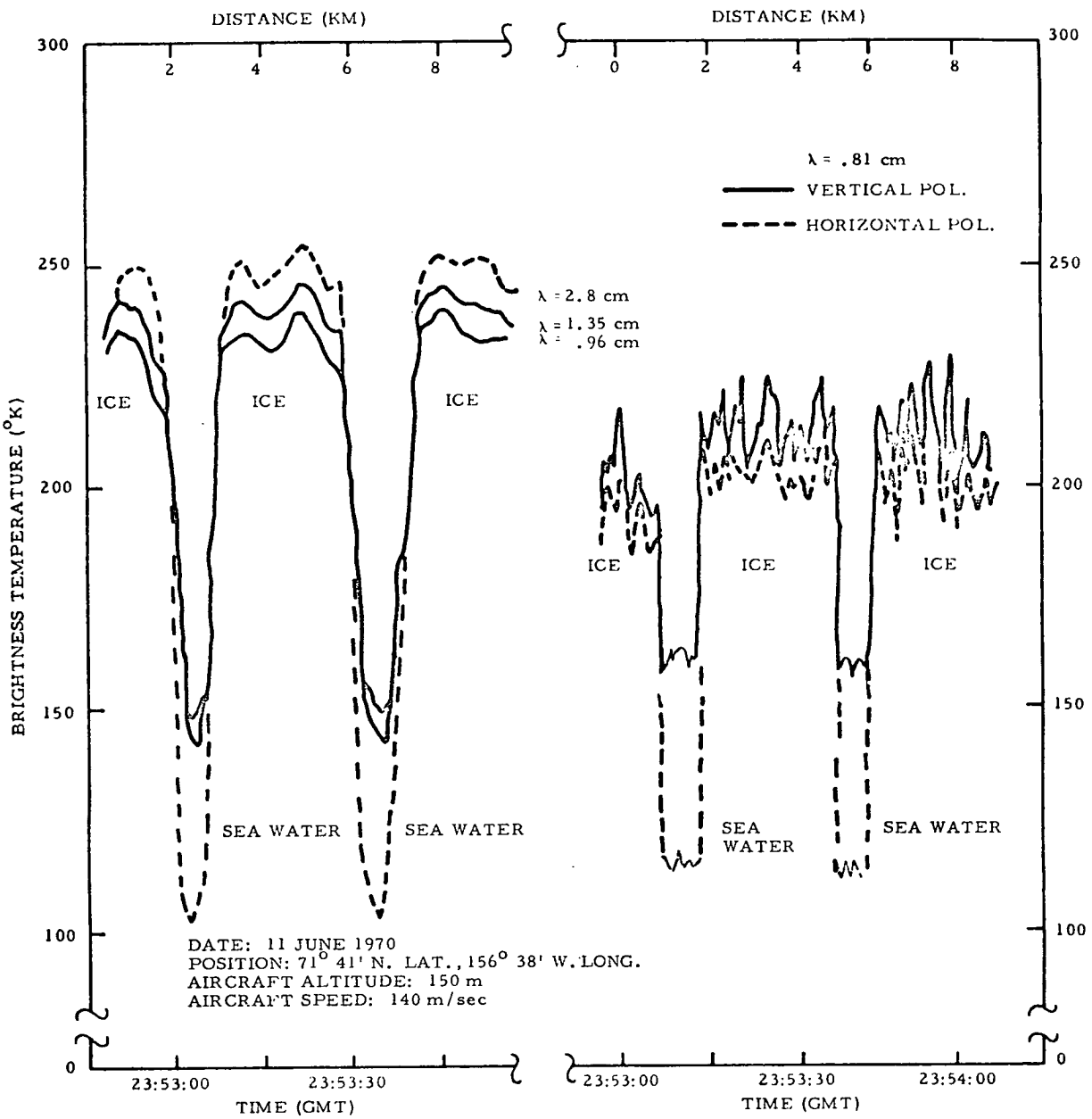

Figure 2. Typical Brightness Temperature Profile Across Ice and Sea Water.

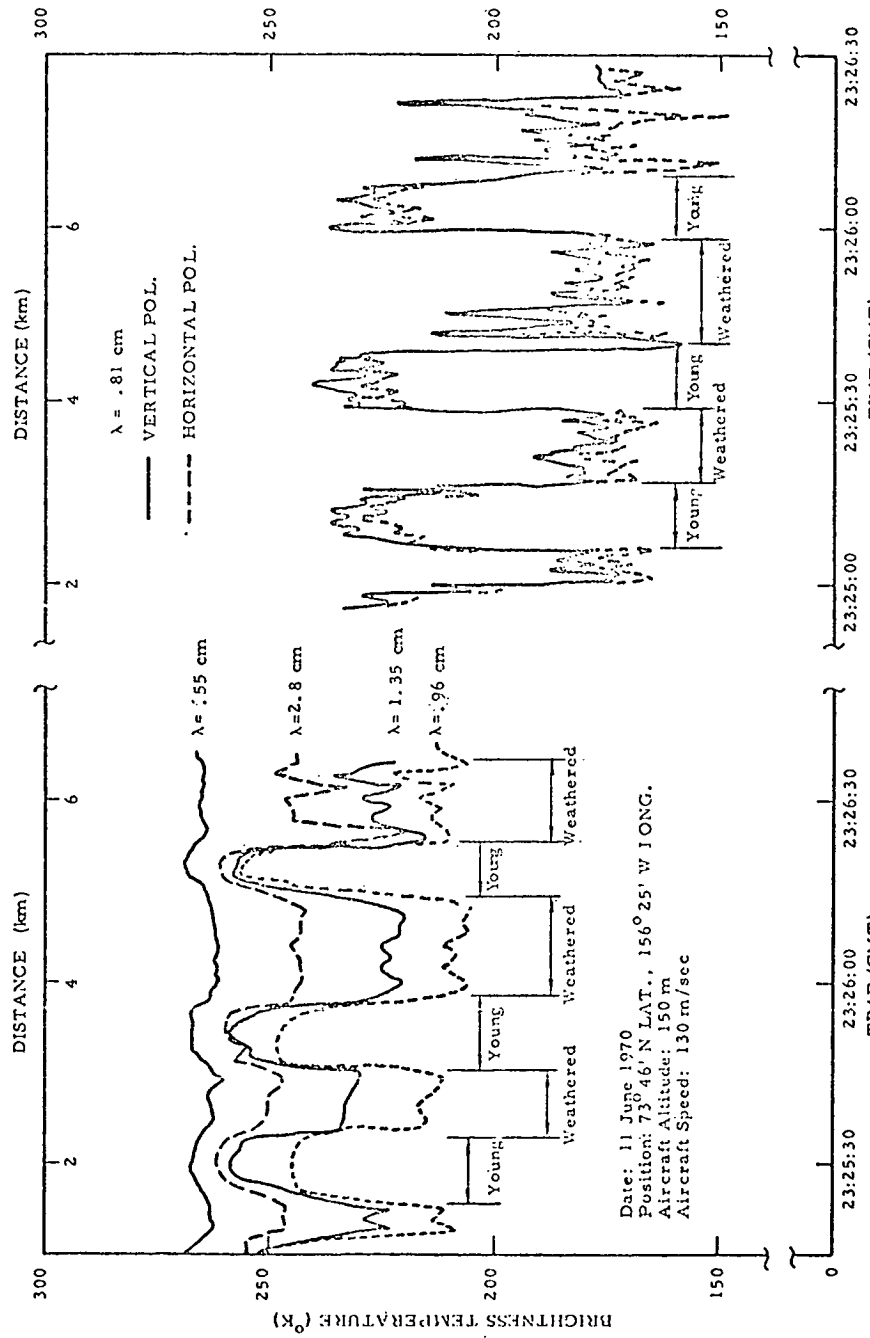

Figure 3. Typical Brightness Temperatures of "Young" and "Weathered" Ice Types

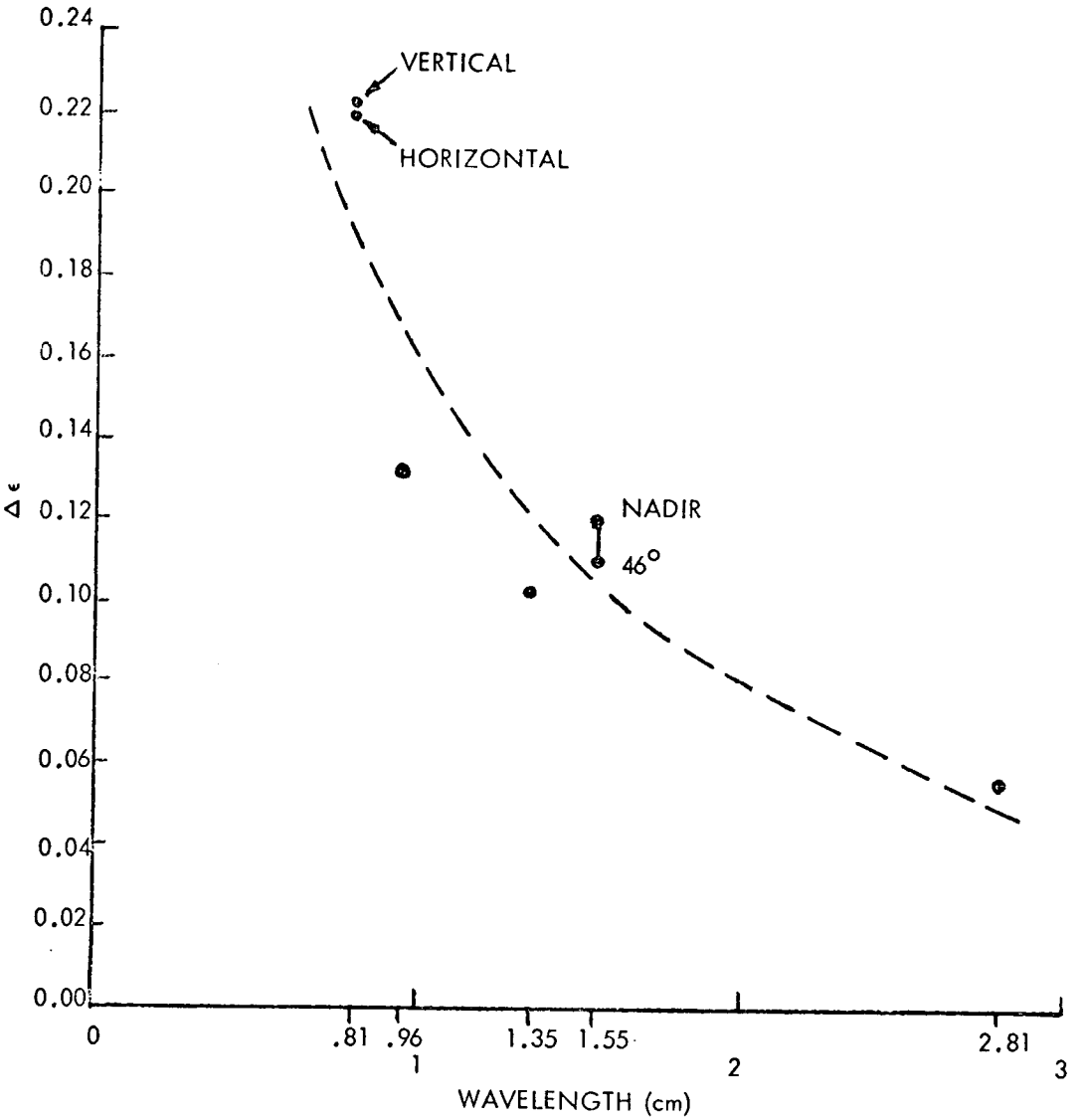

Figure 4. Change in Emissivity $\Delta\varepsilon$ for Two Ice Types Versus Observational Wavelength.

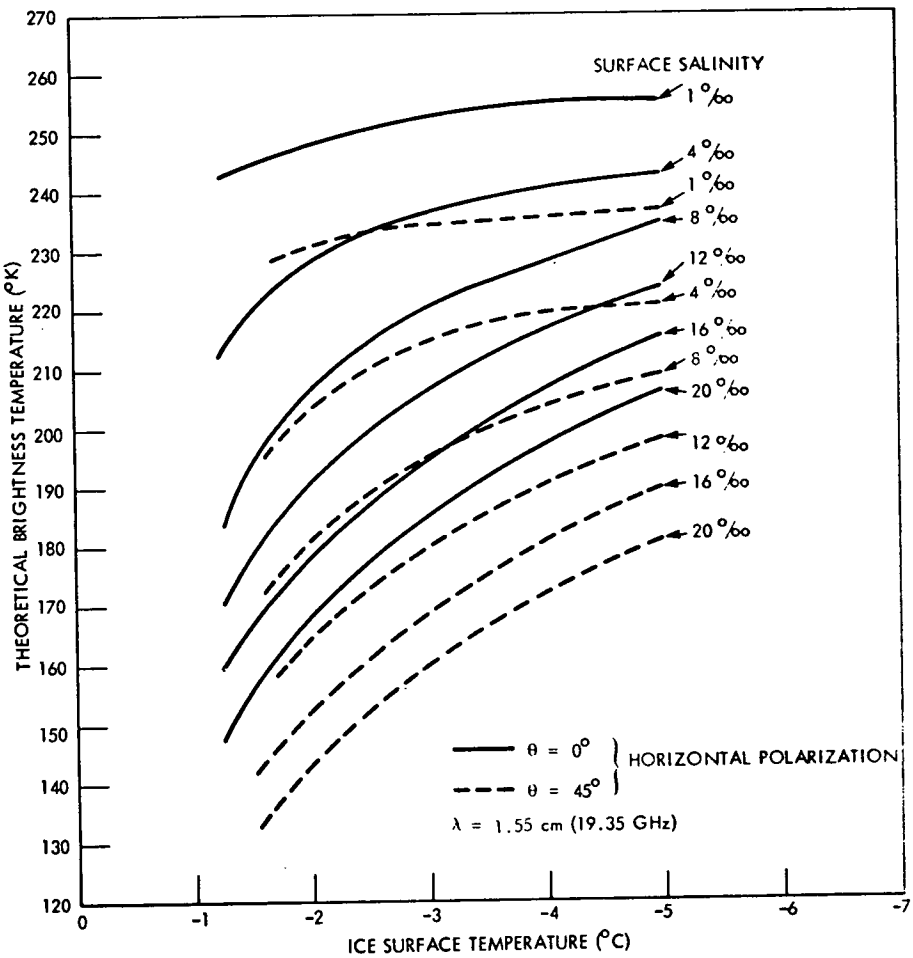

Figure 5. Brightness Temperature versus Ice Surface Temperature for Various Surface Salinities (λ = 1.55 cm)

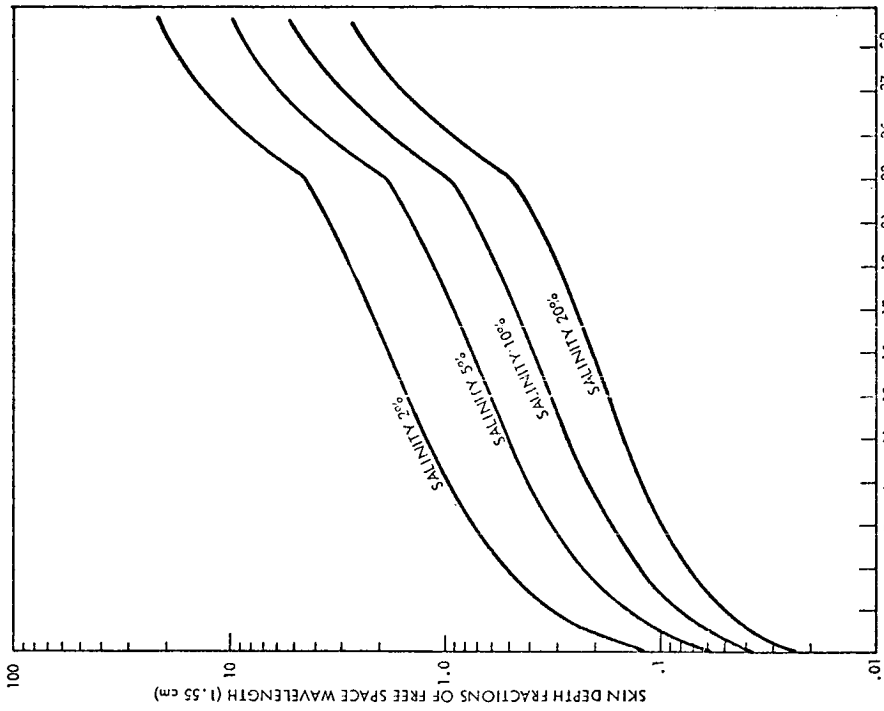

Figure 7. Skin Depth versus Sea Ice Temperature for Various Brine Concentrations, λ = 1.55 cm

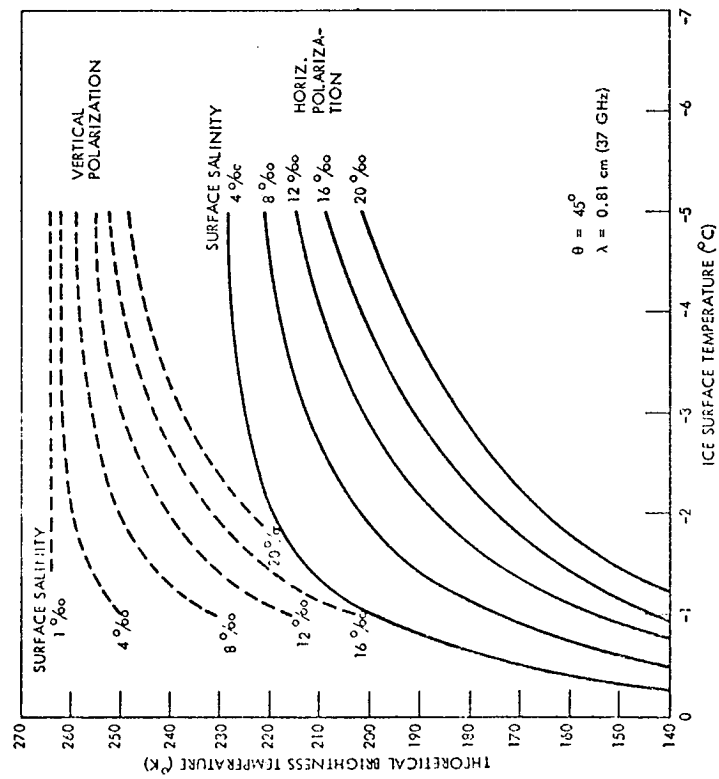

Figure 6. Brightness Temperature versus Ice Surface Temperature for Various Surface Salinities (λ = 8.1 mm)